Supporting information

The rational design of specific SOD1 inhibitors via copper-coordination and their application in ROS signaling research

Xiongwei Dong,‡ Zhe Zhang,‡ Jidong Zhao, Juan Lei, Yuanyuan Chen, Xiang Li, Huanhuan Chen, Junli Tian, Dan Zhang, Chunrong Liu,* Changlin Liu*

‡ These authors contributed equally.

* Correspondence: liucr@mail.ccnu.edu.cn，liuchl@mail.ccnu.edu.cn

Table of contents **page**

Experimental method and instrumentation

Characterization. The chelators were prepared and characterized according to the reported procedure [1-3], details could be found in the Supplementary Information (Synthesis and characterization). The crystals of chelators and these Cu^{2+} complexs suitable for X-ray diffraction were sealed in a thin-walled quartz capillariy and mounted on a Bruker AXS Smart 1000 CCD Diffractometer equipped with graphite-monochromated Mo-Ka or Cu-Ka radiation (λ = 0.71073 Å) at 298K. The structures were resolved with direct methods and multi-scan absorption corrections were applied using the $SAINT^{+}$ program. The final refinement was performed with SHELXL-97 by full-matrix least-squares methods on F^2 with anisotropic thermal parameters for non-hydrogen atoms. All non-hydrogen atoms were refined anisotropically to convergence. All hydrogen atoms were added in the theoretically calculated positions and refined isotropically with fixed thermal factors (U_{iso}(H) = 1.2 U_{eq} (aromatic, methylene C and imine N atoms), U_{iso}(H) = U_{eq} (methyl C)). The disordered solvent molecules were treated with the program Squeeze/Platon, and their distributions were subtracted.

Determination of acidity and stability constants. Acidity constants (pK_a) of the chelators and stability constant (pK) of the M^{2+}-complexes (M = Cu, Mn, Zn and Fe) were determined by potentiometric titrations. Potentiometric titrations were performed with a Metrohm 877 Titrino Plus automated titrator equipped with a Metrohm 6.0262.100 glass electrode calibrated against standard buffers. The water-jacketed titration vessel was maintained at 25.0 ℃ (± 0.5 ℃). To estimate pK_a values, chelators were predissolved in excess of HNO_3 (1.0 mM) and diluted with water [10% (vol/vol) DMSO] in the titration vessel (25.0 mL), the final concentrations of HNO_3 and chelators were 100 μM. All measurements were conducted in the presence of 100 mM KNO_3 to maintain constant ionic strength. Solutions were titrated with 75.5 mM NaOH, which was prepared with degassed water and standardized with Potassium biphthalate prior to each titration. Data analysis was carried out with the program HyperQuad 2013 (Protonic Software, UK) [4, 5]. The stability constant of M^{2+}-complex was determined by the titrations performed in the presence of 1.0 equiv of 100.0 μM metal nitrates using the pK_a values determined above. Species

distribution plots and titration simulations were built with the program HySS2009 (Protonic Software) [6, 7]. The data represented here were the mean ± SD of the results obtained from at least three independent measurements.

Electrochemical measurement. Cyclic voltammograms were recorded with a CH instruments Electrochemical Analyser equipped with Chi600E software employing a glassy carbon working electrode, platinum wire auxiliary electrode, and Ag/Ag^{+} reference electrode. All measurements were carried out in DMF and 2 mM of analyte was dissolved in the 0.1 M sodium perchlorate solution. Each solution was purged with nitrogen prior to analysis and measured at ambient temperature. Each sample was referenced to an internal reference of ferrocene, which was taken as having a $E_{1/2}$ = 0.56 V in DMF versus SCE.

Fluorescence measurement. All fluorescence measurements were performed in 10 mM Tris-buffer, pH 7.4, on a Cary Eclipse fluorescence spectrophotometer (Varian, USA) at 25 ℃. The fluorescence emission spectra of LD**94** and LD**100** were collected between 400 and 680 nm, and the excitation wavelength of LD**94** and LD**100** was set at 345 and 355 nm, respectively.

Molecular docking simulation. The molecular simulation on docking ligands into the 3D structures (http://www.rcsb.org) of the proteins SOD1 (PDB: 1CBJ) and tyrosinase (PDB: 4P6T) was carried out using the program suite AutoDock 4.2.0 (http://autodock.scripps.edu). The widely used Lamarckian Genetic Algorithm (LGA) [8,9] was chosen for the docking calculation. AutoDockTools (ADT 1.4.6) was performed to setup each ligand-protein interaction, where all hydrogen atoms were added, Gasteiger charges were calculated and nonpolar hydrogen atoms were merged to carbon atoms. The solvent molecules were removed from the protein 3D structures to obtain the docking grid, and the active site was defined using AutoGrid. The grid size was set to 60 *60 * 60 points with grid spacing of 0.375 Å, *van der* Waals well depth of 0.100 kcal/mol, an iteration of 200 [10] and a population size of 100. The grid box was centered on the center of the ligand from the corresponding protein structures. Formal structures of the ligands were assigned by the program SYBYL, and the best ranked pose was selected from the ChemScore. The conformation with the lowest binding energy was used to analyze ligand placement. Electrostatic potential for the Cu^{2+} complexes were calculated in methanol phase with a single point calculation at a density functional theory (DFT) level using the B3LYP exchange-correlation functional. Considering both the calculation cost and the accuracy, the

LACVP** basis set was used, which corresponds to the "double-ξ" basis set with polarization functions 6-31G(d, p) [11] for N, O, Cl and S, whereas for Cu the pseudo potential LanL2DZ [12] was used. All calculations were done with the GAMESS suite of codes [13].

Cell culture. HeLa and Cos-7 cell lines were purchased from China Center for Type Culture Collection. Hela cells and Cos-7 cells were cultured in Dulbecco's modified Eagle medium (DMEM, Invitrogen), supplemented with 10% fetal bovine serum (FBS, Invitrogen). DU145 cells were cultured in Iscove's modified Dulbecco's medium (IMDM, Invitrogen) supplemented with 10% fetal bovine serum (FBS, Invitrogen).

Confocal imaging. All confocal imaging experiments were carried out with a Carl Zeiss laser scanning confocal microscope (Carl Zeiss, Germany). The serum starved Hela cells were co-cultured with 50μM of LD**94** or LD**100** for 4 h, and then washed by 1 mL PBS for three times. Hela cells were imaged by two-photon excitation at 700 nm for LD**94** and 710 nm for LD**100**. Data were analyzed by the software package attached to this instrument.

Cytotoxicity Assay. Cytotoxicity of the chelators was evaluated by MTT assay. Briefly, after HeLa cells reached 80% confluence in 96-well plates, the FBS-containing medium was replaced with a FBS-free medium. After incubation for 24 h in the medium, the chelators were added (varied concentrations) into the wells (6 parallel wells tested). Following further incubation for 24 h at 37 ℃, 20 μL of MTT (5 mg/mL) in PBS was added to the wells. After incubated for 4 h, the MTT-containing medium was replaced by 200 μL DMSO. The 96-well plates were oscillated for 10 min to fully dissolve the formazan crystal formed by living cells. The relative viability of cells in each well was determined by measuring the absorbance at 490 nm of each well by a SpectraMax M5 Microplate Reader. Non-treated cells (in DMEM) were used as a control and the relative cell viability of each of the LD-treated cells (mean% ± SD, n=3) was expressed as OD_{sample} / $OD_{control}$ * 100%.

Analysis of Binding Parameters Using Fluorescence Anisotropy. The anisotropy (*r*) was calculated by the instrument software; as classically reported: [14]

$$r = \frac{I_{vv} - GI_{vh}}{I_{vv} + 2GI_{vh}} \qquad (1)$$

I_{vv} and I_{vh} were the vertically and horizontally polarized components of the emission after excitation by vertically polarized light. The instrumental correction factor G was determined from

standard solutions according to the manufacturer's instructions. We took into consideration the fact that the protein (*P*, SOD1) is not in very large excess compared to ligand (*L*, **LD100**). The equilibrium constant is expressed by the following equation:

$$K = \frac{[L_n P]}{[L]^n [P]} \qquad (2)$$

The measured anisotropy *r* can be linked to the apparent binding constant *K* via the following relation as described by literature [15,16]

$$K = \frac{C_L . f_B / n}{\left[C_L(1 - f_B)\right]^n (C_P - C_L . f_B / n)} \qquad (3)$$

$$f_B = \frac{n[L_n P]}{n[L_n P] + [L]} = \frac{r - r_L}{(r_{L_n P} - r)R + r - r_L}, \quad R = \frac{f_B}{f_F} = \frac{F_B}{F_F} \qquad (4)$$

where C_L is the concentration of ligand (**LD100**), C_p is the concentration of protein (SOD1), r is the average anisotropy of reaction system, $r_{L_n P}$ is the anisotropy of maximally ligand-associated protein, r_L is the anisotropy of free ligand, F_F and F_B are the fluorescence intensity of free ligand and protein bonding ligand, respectively. In equation (3) we simply invert this probability and take its log:

$$lgf_B - n\lg\left(1 - f_B\right) = lgK + (n-1)lgc_L + lgn + lg(C_p - C_L . f_B / n) \qquad (5)$$

For a 1:1 stoichiometry (n=1), a standard linear equation has two parameters that should be estimated based on the X (define $lg\left(C_p - C_L . f_B\right)$) and Y (define $lgf_B - \lg\left(1 - f_B\right)$) plots provided, which are the slope (if n=1, the slope of this linear fitting equation be close to 1.0) and Y intercept (lgK).

REFERENCES

1. F. E. Anderson, C. J. Duca, J. V. Scudi, *J. Am. Chem. Soc.,* 1951, **73**, 4967–4968.

2. A. Nohara, T. Umetani, Y. Sanno, *Tetrahedron Lett.,* 1973, **14**, 1995–1998.

3. S. Hossain, S. Das, A. Chakraborty, F. Lloret, J. Cano, E. Pardo, V. Chandrasekhar, *Dalton Trans.,* 2014, **43**, 10164–10174.

4. P. Gans, A. Sabatini, A. Vacca, *Ann. Chim.* 1999, **89**, 45–49.

5. P. Gans, A. Sabatini, A. Vacca, *Talanta.,* 1996, **43**, 1739–1753.

6. L. Alderighi, P. Gans, A. Ienco, D. Peters, A Sabatini, A. Vacca, *Coord. Chem. Rev.,* 1999, **184**, 311–318.

7. J. A. Thomas, R. N. Buchsbaum, A. Zimniak, E. Racker, *Biochemistry.,* 1979, **18**, 2210–2218.

8. G. M. Morris.; D. S. Goodsell, R. S. Halliday, R. Huey, W. E. Hart, R. K. Belew, A. J. Olson, *J. Comput. Chem.,* 1998, **19**, 1639–1662.

9. N. Brooijmans, I. D. Kuntz, *Annu. Rev. Biophys. Biomol. Struct.,* 2003, **32**, 335–373.

10. G. M. Morris. D. S. Goodsell, R. Huey, A. J. Olson, *J. Comput. Aide Mol. Des.* 1996, **10**, 293–304.

11. M. M. Francl, W. J. Pietro, W. J. Hehre, J. S. Binkley, M. S. Gordon, D. J. DeFrees, J. A. Pople, *J. Chem. Phys.* 1982, **77**, 3654–3665.

12. P. J. Hay, W. R. Wadt, *J. Chem. Phys.* 1985, **82**, 299–310.

13. M. W. Schmides, K. K. Baldridge, J. A. Boau, J. H. Jensen, S. Koseki, M. S. Grodon, S. T. Elbert, *J. Comput. Chem*, 1993, **14**, 1347–1363.

14. J. R. Lakowicz, Principles of Fluorescence Spectroscopy, *Springer Science: New York*, 2007; **Chapter 10**.

15. J. W. G. Visser A., J. Lee, *Biochemistry*, 1980, 19, 4366–4372.

16. N. A. Carmona, B. Cohen, J. A. Organero, et al. *J. Photoch. Photobio. A: Chemistry*, 2012, **234**, 3–11.

17. F. E. Anderson, C. J. Duca, J. V. Scudi, *J. Am. Chem. Soc.* 1951, **73**, 4967–4968.

18. A. Nohara, T. Umetani, Y. Sanno, *Tetrahedron Lett.* 1973, **14**, 1995–1998.

19. S. Hossain, S. Das, A. Chakraborty, F. Lloret, J. Cano, E. Pardo, V. Chandrasekhar, *Dalton Trans.* 2014, **43**, 10164–10174.

20. L. Banci, I. Bertini, S. Ciofi-Baffoni, T. Kozyreva, K. Zovo, P. Palumaa, *Nature*, 2010, **465**, 645–648.

Synthesis and characterization

LD18, **LD25**, **LD27**, **LD29** and **LD34** were synthesized by following the reported procedure with slight modification (Ref. 17).

General procedure: 2-pyridinecarboxaldehyde, salicylaldehyde, 5-chloro-salicylaldehyde or 3-carbaldehyde chromone (10 mmol) were mixed with corresponding thioureido derivatives including thiosemicarbazide (for **LD18**, **LD29** and **LD34**, 10 mmol, in 10 ml water), 4-methyl-3-thiosemicarbazide (for **LD25**, 10 mmol) , semicarbazide (for **LD27**, 10 mmol, in 10 ml water) in 1:1 molar ratio, and then a catalytic amount of acetic acid in alcohol (30 ml) was added. The mixture was refluxed for 3-6 h, cooled, and the solvent was evaporated. The ligands were isolated by column chromatography or purified by recrystallization.

Data for **LD18**: yield 1.52 g (85%); slight yellow crystals; ESI-MS: m/z 181.20 ($M\text{-}H^+$)，calculated：181.23；^{1}H NMR (400 MHz, DMSO) δ 8.45 (t, *J* = 12.1 Hz, 1H), 8.05 (d, *J* = 9.0 Hz, 2H), 7.72 (dd, *J* = 25.7, 18.3 Hz, 1H), 7.29 – 7.11 (m, 1H).^{13}C NMR (400 MHz, DMSO) δ 178.39, 153.29, 149.29, 142.63, 136.51, 124.11, 120.21.

Data for **LD25**: yield 1.50 g (78%); white solid; ESI-MS: m/z 195.20 ($M\text{-}H^+$)，calculated：195.25；^{1}H NMR (400 MHz, DMSO) δ 11.70 (s, 1H), 8.66 (s, 1H), 8.55 (s, 1H), 8.25 (d, *J* = 7.4 Hz, 1H), 8.09 (s, 1H), 7.83 (d, *J* = 6.5 Hz, 1H), 7.56 – 7.21 (m, 1H), 3.03 (s, 3H). ^{13}C NMR (400 MHz, $CDCl_3$) δ 177.92, 153.43, 149.35, 141.95, 136.49, 124.04, 120.08, 30.94.

Data for **LD27**: yield 1.12 g (68%); white crystals; ESI-MS: m/z 165.25 ($M\text{-}H^+$)，calculated：165.18；^{1}H NMR (400 MHz, DMSO) δ 11.34 (s, 1H), 8.76 (d, *J* = 4.2 Hz, 1H), 8.52 (s, 1H), 8.29 (d, *J* = 7.8 Hz, 1H), 8.06 (s, 1H), 7.88 (s, 1H), 7.60 (s, 1H), 6.86 (s, 1H). ^{13}C NMR (400 MHz, DMSO) δ 156.02, 146.76, 145.93, 142.31, 129.46, 125.60, 125.26.

Data for **LD29**: yield 1.32 g (69%); white crystals; ESI-MS: m/z 196.20 ($M\text{-}H^+$)，calculated：

196.24；^{1}H NMR (600 MHz, DMSO) δ 11.39 (s, 1H), 9.89 (s, 1H), 8.37 (s, 1H), 8.12 (s, 1H), 7.92 (d, *J* = 7.0 Hz, 2H), 7.20 (d, *J* = 7.2 Hz, 1H), 6.86 (d, *J* = 8.2 Hz, 1H), 6.80 (t, *J* = 7.5 Hz, 1H). ^{13}C NMR (400 MHz, DMSO) δ 177.71, 156.53, 140.14, 131.34, 126.97, 120.35, 119.50, 116.23.

Data for **LD34**: yield 1.72 g (73%); white crystals; ESI-MS: m/z 230.15 (M-H^{+})，calculated：230.69；^{1}H NMR (400 MHz, DMSO) δ 11.47 (s, 1H), 10.23 (s, 1H), 8.35 (s, 1H), 8.15 (d, *J* = 26.7 Hz, 2H), 8.11–7.94 (m, 1H), 7.23 (d, *J* = 8.7 Hz, 1H), 6.90 (d, *J* = 8.7 Hz, 1H). ^{13}C NMR (400 MHz, DMSO) δ 177.87, 155.16, 137.50, 130.42, 125.48, 123.51, 122.35, 117.72.

LD61, **LD72**, **LD74**, **LD81**, **LD82**, **LD83** and **LD84**: chromone-3-carboxaldehyde, quinoline-2-carboxaldehyde and 8-hydroxyquinoline-2-carboxaldehyde were prepared according to the literature methods (Online Method, Ref. 18, 19).

General procedure: Chromone-3-carboxaldehyde, quinoline-2-carboxaldehyde or 8-hydroxyquinoline-2-carboxaldehyde (10 mmol) were mixed with corresponding primary amine including thiosemicarbazide (for **LD61**, **LD81** and **LD83**, 10 mmol, in 10 ml water), 4-methyl-3-thiosemicarbazide (for **LD72**, 10 mmol, in 10 ml alcohol), 2-aminophenol (for **LD74**, 10 mmol, in 10 ml alcohol), semicarbazide (for **LD82** and **LD84**, 10 mmol, in 10 ml water) in 1:1 molar ratio, and then a catalytic amount of acetic acid in alcohol (30-50 ml) was added and the mixture was refluxed for 3-6 h. Then, the mixture was cooled and concentrated and purified by column chromatography or recrystallization to afford products.

Data for **LD61**: yield 1.35 g (56%); white solid; ESI-MS: m/z 248.20 (M-H^{+})，calculated：248.27；^{1}H NMR (400 MHz, DMSO) δ 11.55 (s, 1H), 9.14 (s, 1H), 8.28 (s, 1H), 8.17 (s, 1H), 8.11 – 7.97 (m, 2H), 7.81 (t, *J* = 7.1 Hz, 1H), 7.68 (d, *J* = 8.3 Hz, 1H), 7.51 (t, *J* = 7.0 Hz, 1H). ^{13}C NMR (400 MHz, DMSO) δ 178.01, 174.77, 155.70, 155.19, 134.50, 134.01, 126.00, 125.16, 123.32, 118.72, 118.31.

Data for **LD72**: yield 1.21 g (46%); slight yellow crystals; ESI-MS: m/z 262.20 (M-H^{+})，calculated：262.30；^{1}H NMR (400 MHz, dmso) δ 11.61 (s, 1H), 9.11 (s, 1H), 8.57 (s, 1H), 8.28 – 8.05 (m, 2H), 7.83 (t, *J* = 7.5 Hz, 1H), 7.71 (d, *J* = 8.2 Hz, 1H), 7.52 (t, *J* = 7.1 Hz, 1H), 3.01 (d, *J* = 3.5 Hz, 3H). ^{13}C NMR (400 MHz, DMSO) δ 177.72, 174.78, 155.73, 154.88, 134.53, 133.40, 126.02, 125.18, 123.34, 118.75, 118.42, 30.71.

Data for **LD74**: yield 1.81 g (71%); white solid; ESI-MS: m/z 266.20 ($M-H^+$)，calculated：266.28；^{1}H NMR (400 MHz, DMSO) δ 10.32 (s, 1H), 8.15 (d, *J* = 13.0 Hz, 1H), 7.85 (d, *J* = 7.5 Hz, 1H), 7.55 – 7.43 (m, 2H), 7.12 (dd, *J* = 19.8, 7.8 Hz, 2H), 6.91 (d, *J* = 30.1 Hz, 3H), 5.84 (s, 1H). ^{13}C NMR (400 MHz, DMSO) δ 179.42, 155.29, 146.04, 144.20, 134.13, 127.65, 125.56, 124.27, 122.88, 121.91, 119.85, 117.94, 115.53, 114.08, 103.15, 101.29.

Data for **LD81**: yield 1.30 g (58%); slight yellow solid; ESI-MS: m/z 231.20 ($M-H^+$)，calculated：231.29；^{1}H NMR (400 MHz, DMSO) δ 11.87 (s, 1H), 8.44 (dd, *J* = 32.9, 24.3 Hz, 3H), 8.34 – 8.16 (m, 2H), 8.03 (s, 1H), 7.96 (dd, *J* = 29.7, 8.0 Hz, 2H), 7.72 (t, *J* = 7.1 Hz, 1H), 7.56 (d, *J* = 7.2 Hz, 1H). ^{13}C NMR (400 MHz, DMSO) δ 178.48, 153.81, 147.16, 142.43, 136.44, 130.01, 128.64, 127.93, 127.82, 127.18, 118.14.

Data for **LD82**: yield 1.90 g (79%); yellow solid; ESI-MS: m/z 215.20 ($M-H^+$)，calculated：215.09；^{1}H NMR (600 MHz, DMSO) δ 11.52 (s, 1H), 8.92 (d, *J* = 7.5 Hz, 1H), 8.64 (d, *J* = 8.7 Hz, 1H), 8.50 (s, 1H), 8.32 (s, 1H), 8.23 (d, *J* = 8.0 Hz, 1H), 8.04 (t, *J* = 7.5 Hz, 1H), 7.84 (t, *J* = 7.4 Hz, 1H), 7.43 (s, 1H), 6.96 (s, 1H).^{13}C NMR (400 MHz, DMSO) δ 166.18, 150.20, 149.66, 142.89, 133.29, 129.25, 127.25, 126.50, 125.71, 125.12, 116.02.

Data for **LD83**: yield 1.71 g (76%); yellow solid; ESI-MS: m/z 247.20 ($M-H^+$)，calculated：247.30；^{1}H NMR (400 MHz, DMSO) δ 11.88 (s, 1H), 9.87 (s, 1H), 8.44 (d, *J* = 9.0 Hz, 2H), 8.34 (s, 1H), 8.27 (d, *J* = 8.5 Hz, 2H), 7.39 (dd, *J* = 18.3, 7.6 Hz, 2H), 7.09 (d, *J* = 7.2 Hz, 1H). ^{13}C NMR (400 MHz, DMSO) δ 178.43, 153.45, 151.87, 142.43, 138.17, 136.19, 128.82, 128.13, 118.47, 117.80, 112.16.

Data for **LD84**: yield 1.73g (74%); yellow solid; ESI-MS: m/z 231.20 ($M-H^+$)，calculated：231.10；^{1}H NMR (600 MHz, DMSO) δ 11.49 (s, 1H), 8.90 (d, *J* = 7.5 Hz, 1H), 8.62 (d, *J* = 8.7 Hz, 1H), 8.48 (s, 1H), 8.30 (s, 1H), 8.21 (d, *J* = 8.0 Hz, 1H), 8.02 (t, *J* = 7.5 Hz, 1H), 7.82 (t, *J* = 7.4 Hz, 1H), 7.45 (d, *J* = 44.0 Hz, 1H), 6.94 (s, 1H). ^{13}C NMR (400 MHz, DMSO) δ 155.96, 150.22, 149.21, 143.00, 132.24, 129.61, 128.75, 118.74, 118.25, 115.73.

Synthesis of **LD93**, **LD94** and **LD100**, a water solution of thiocarbohydrazide was added dropwise to the solution of 2-pyridinecarboxaldehyde (for **LD93**), salicylaldehyde (for **LD94**) or 5-chlorosalicylaldehyde (for **LD100**) in ethanol at 60-70℃. Then, the mixture was refluxed for 4 hours and a large amount of precipitate was observed. Then the mixture was cooled to room temperature and filtrated to gain white solids. The solids were washed with methanol and DI

water, and then dried with vacuum to get the intermediate. Then the intermediate was added to an ethanol solution containing chromone-3-carboxaldehyde in 1:1 molar ratio. The yellow precipitate was formed after refluxed for 4 hours and isolated by filtration, washed with water and methanol. The crude product ware recrystallized from water/DMF or water/DMSO.

Data for **LD93**: yield 1.88 g (54%); yellow solid; ESI-MS: m/z 352.20 ($M-H^+$)，calculated：352.09；^{1}H NMR (600 MHz, DMSO) δ 12.25 (d, *J* = 66.9 Hz, 1H), 11.74 (s, 1H), 9.27 (s, 1H), 8.79 (d, *J* = 55.0 Hz, 1H), 8.62 (s, 1H), 8.31 (d, *J* = 16.9 Hz, 1H), 8.12 (d, *J* = 23.9 Hz, 2H), 7.88 (dt, *J* = 15.6, 7.6 Hz, 2H), 7.74 (d, *J* = 7.9 Hz, 1H), 7.55 (t, *J* = 7.5 Hz, 1H), 7.48 – 7.37 (m, 1H). ^{13}C NMR (400 MHz, DMSO) δ 180.66, 175.24, 158.90, 155.87, 149.84, 149.62, 136.92, 134.29, 130.62, 126.43, 125.33, 123.43, 121.53, 119.32, 118.87, 118.70, 117.36.

Data for **LD94**: yield 1.39 g (42%); slight yellow crystals; ESI-MS: m/z 367.10 ($M-H^+$)，calculated：367.09；^{1}H NMR (400 MHz, DMSO) δ 12.26 (s, 1H), 11.87 (s, 1H), 11.53 (s, 1H), 9.20 (s, 1H), 8.71 (s, 1H), 8.21 (d, *J* = 72.5 Hz, 2H), 7.79 (d, *J* = 42.3 Hz, 2H), 7.65 – 7.16 (m, 3H), 6.94 (s, 2H). ^{13}C NMR (400 MHz, DMSO) δ 180.04, 174.82, 174.53, 157.40, 155.79, 149.36, 136.09, 134.69, 131.42, 126.19, 125.25, 123.39, 122.3, 119.33, 118.82, 118.18, 118.10, 116.70.

Data for **LD100**: yield 2.53 g (66%); yellow crystals; ESI-MS: m/z 401.05 ($M-H^+$)，calculated：401.04；^{1}H NMR (600 MHz, DMSO) δ 12.30 (s, 1H), 11.96 (s, 1H), 11.56 (s, 1H), 9.20 (s, 1H), 8.67 (s, 1H), 8.30 (s, 1H), 8.12 (d, *J* = 7.4 Hz, 1H), 7.85 (t, *J* = 7.6 Hz, 1H), 7.73 (d, *J* = 8.2 Hz, 1H), 7.55 (t, *J* = 7.0 Hz, 2H), 7.32 (d, *J* = 7.6 Hz, 1H), 6.96 (d, *J* = 8.3 Hz, 1H). ^{13}C NMR (400 MHz, DMSO) δ 179.56, 174.11, 173.69, 167.67, 165.82, 152.45, 139.24, 136.35, 133.04, 128.35, 126.01, 124.88, 122.79, 121.58, 121.45, 120.82, 119.84, 118.87.

Synthesis of chelator-Cu(II) complexes: 0.2 mmol of **LD18** (0.036 g), **LD25** (0.039 g), **LD27** (0.039 g), **LD29** (0.040 g) or **LD34** (0.046 g) was dissolved in a methanol or ethanol solution (10 mL), respectively. Then equal $CuSO_4$, $CuCl_2$ or $Cu(NO_3)_2$ were added, the mixtures were stirred for 4-8 at room temperature before being filtered. The filtrate was kept in air for 8-10 days, yielding crystals of complexes. The crystals were isolated, washed three times with DI water and dried in a vacuum desiccator containing anhydrous $CaCl_2$.

Data for **LD18**-Cu(II) complex: dark green crystals; yield 26%; Anal. Calcd for $CuC_7H_8N_4O_4S_2$:

C, 24.74; H, 2.37; N, 16.49. Found: C, 24.47; H, 2.45; N, 16.17.

Data for **LD25**-Cu(II) complex: brown crystals; yield 35%; Anal. Calcd for $CuC_8H_9N_4O_4S_2$: C, 27.23; H, 2.57; N, 15.88. Found: C, 27.59; H, 2.90; N, 16.21.

Data for **LD27**-Cu(II) complex: dark green crystals; yield 46%; Anal. Calcd for $Cu_2C_{14}H_{16}Cl_2N_8O_5 \cdot 2(NO_3)$: C, 25.86; H, 2.48; N, 21.54. Found: C, 25.99; H, 2.39; N, 21.35.

Data for **LD29**-Cu(II) complex: dark green crystals; yield 51%; Anal. Calcd for $Cu_2C_{16}H_{16}N_6O_2S_2 \cdot 2(NO_3)$: C, 30.05; H, 2.52; N, 17.52. Found: C, 30.17; H, 2.21; N, 17.55.

Data for **LD34**-Cu(II) complex: dark green crystals; yield 43%；Anal. Calcd for $CuC_8H_9ClN_3O_2S \cdot NO_3 \cdot CH_4O$: C, 26.74; H, 3.24; N, 13.86. Found: C, 26.57; H, 3.14; N, 14.21.

Supporting information Table 1: The acidity constants (pK_{a1} to pK_{a4}) of chelators determined by potentiometric titrations at 25 ℃ (I = 0.1 M KNO_3). The acidity constants expressed by equation pKa = logβ(H_nL) – logβ($H_{n-1}L$).

Chelators	pK_{a1}	pK_{a2}	pK_{a3}	pK_{a4}
LD18	2.06 ± 0.15	3.64 ± 0.24	11.32 ± 0.15	/
LD25	2.72 ± 0.10	3.42 ± 0.03	11.44 ± 0.21	/
LD27	2.66 ± 0.34	3.95 ± 0.08	11.76 ± 0.11	/
LD29	0.85 ± 0.02	2.34 ± 0.18	8.71 ± 0.02	/
LD34	1.05 ± 0.29	2.56 ± 0.24	8.98 ± 0.13	/
LD93	1.06 ± 0.14	2.26 ± 0.78	3.74 ± 0.07	9.07 ± 0.10
LD94	1.01 ± 0.06	1.17 ± 0.04	2.06 ± 0.21	10.51 ± 0.21
LD100	0.97 ± 0.04	1.72 ± 0.23	2.32 ± 0.21	9.76 ± 0.09

$$LH_4^+ \xrightarrow[-H^+]{pK_{a1}} LH_3 \xrightarrow[-H^+]{pK_{a2}} LH_2^- \xrightarrow[-H^+]{pK_{a3}} LH^{2-} \xrightarrow[-H^+]{pK_{a4}} L^{3-}$$

The small pKa values correspond to the deprotonation of pyridinium and carbonyl oxygen groups, the large pKa values correspond to the deprotonation of amines or sulfhydryls, and the largest pKa value could be assigned to the deprotonation of phenols.

Supporting information Figure 1. Fluorescence spectra of 5 – 50 μM LD100 (up) and the fluorescent response of LD100 (50 μM) to various metal ions (100 μM) (down) in pH 7.4 Tris-buffer (20 mM) containing 1% DMSO (**λex = 355 nm**).

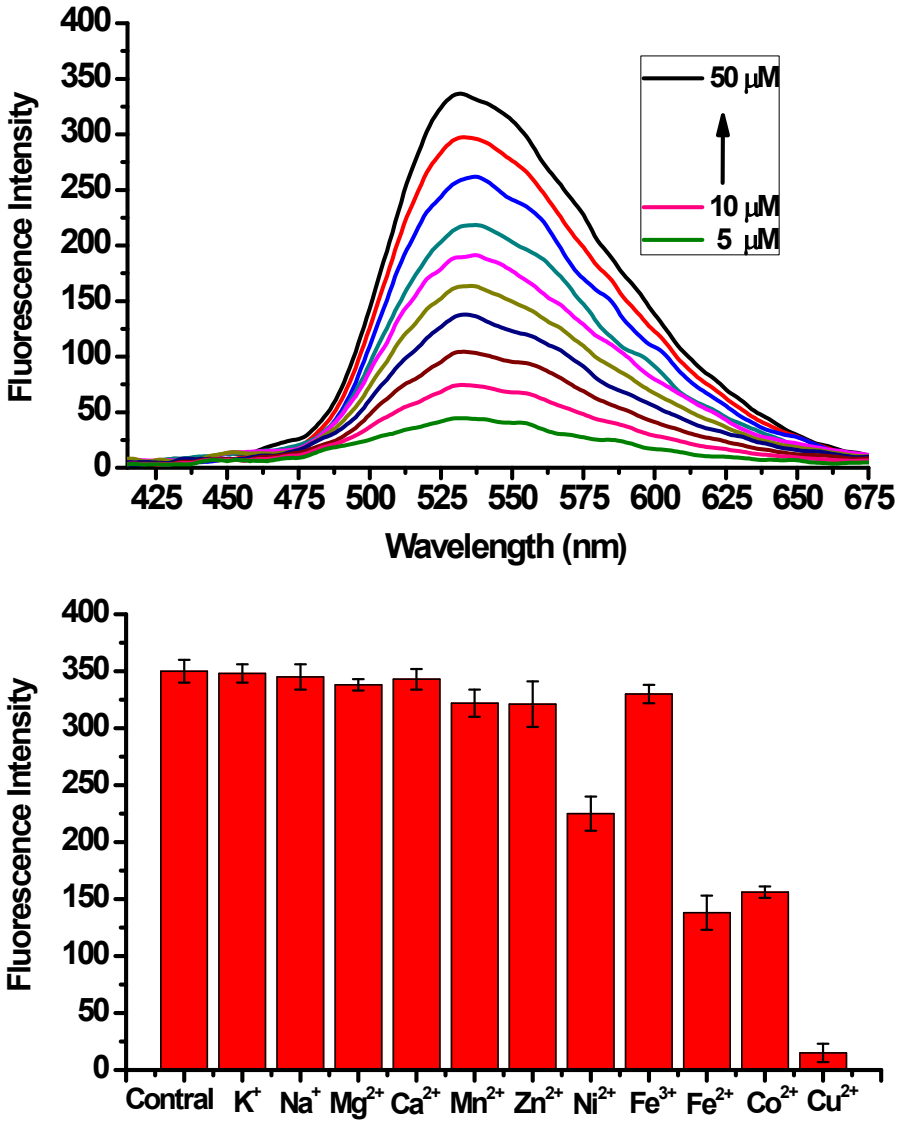

Supporting information Figure 2. Species distribution plots were measured with potentiometric titrations for the Cu^{2+}-chelators systems. Potentiometric titrations were performed for the solutions containing the chelators and equimolar amount $Cu(NO_3)_2$ at 25 ℃ (I = 0.1 M KNO_3).

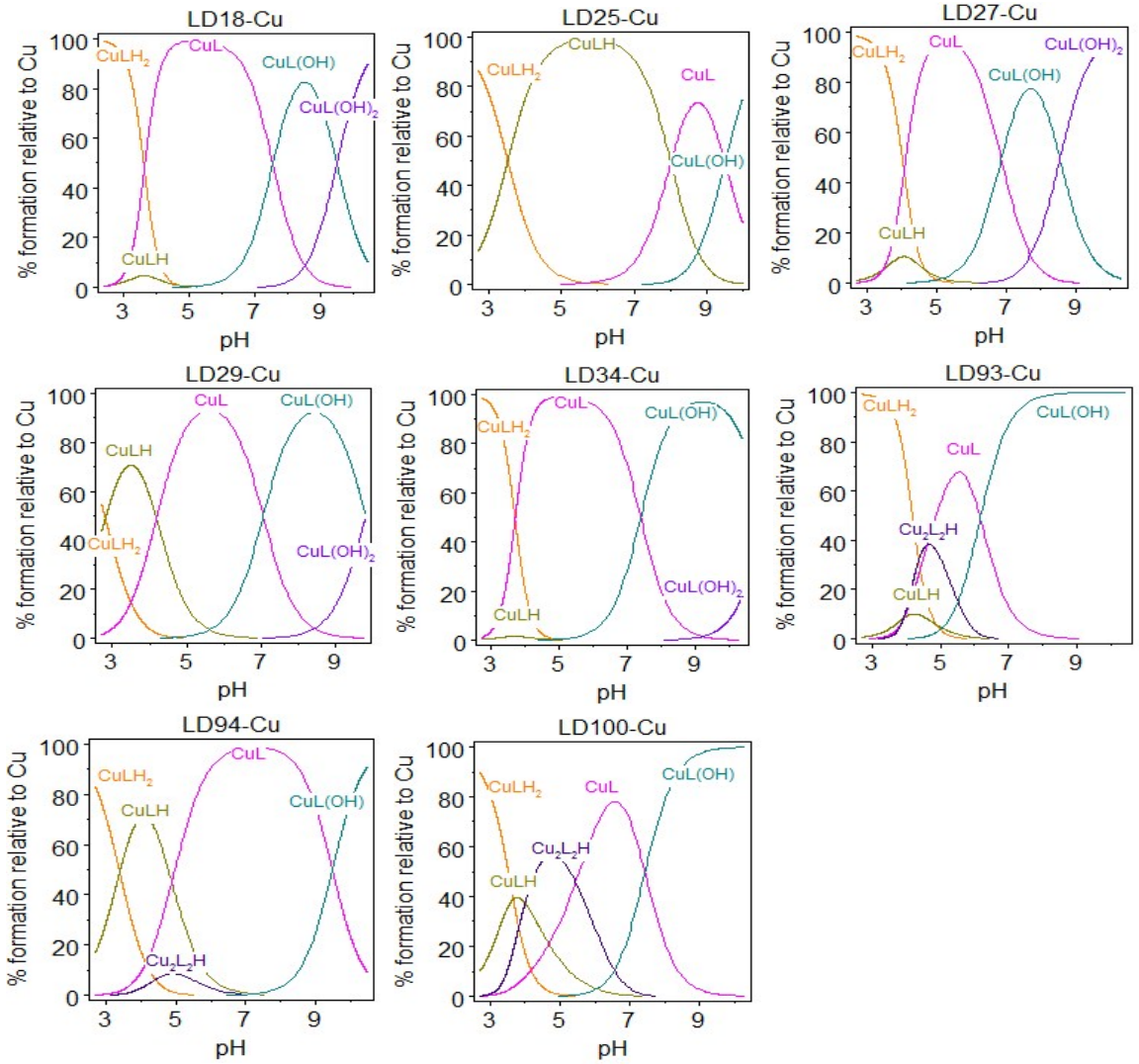

Supporting information Figure 3. X-ray diffraction structures. (a) X-ray diffraction structures of LD18 (CCDC：1030422), LD34 (CCDC：1030421), LD94 (CCDC：1419599) and LD100 (CCDC：1419600). Solvent molecules and counteranions were omitted for clarity, all toms were shown as sphere of arbitrary diameter. **(b)** X-ray diffraction structures of the chelator-Cu^{2+} complexes. LD18-Cu^{2+} complex (CCDC：1423072), LD25-Cu^{2+} complex (CCDC：1031099), LD27-Cu^{2+} complex (CCDC：1030412), LD29-Cu^{2+} complex (CCDC：1031098) and LD34-Cu^{2+} complex (CCDC：1030350). Solvent molecules and counteranions were omitted for clarity, all toms were shown as sphere of arbitrary diameter.

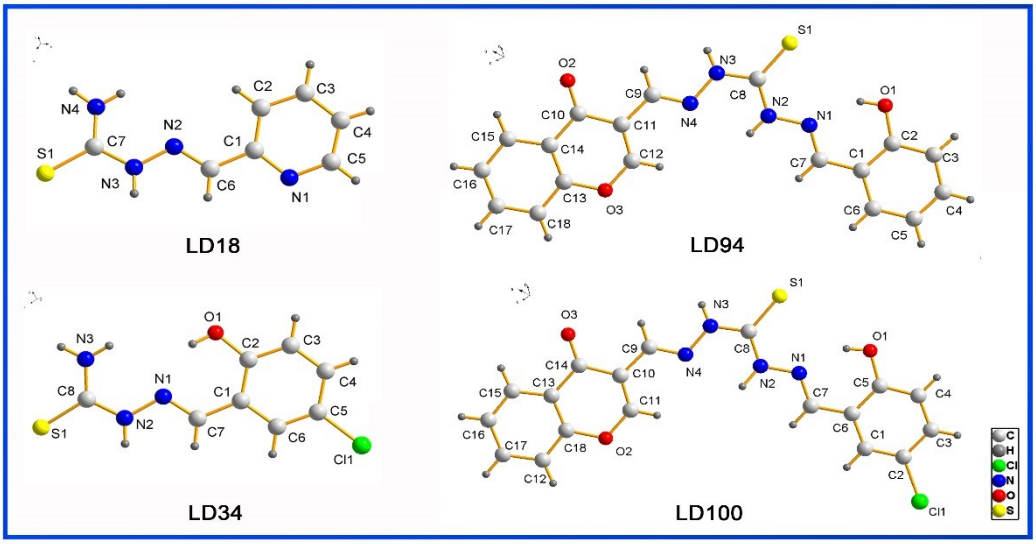

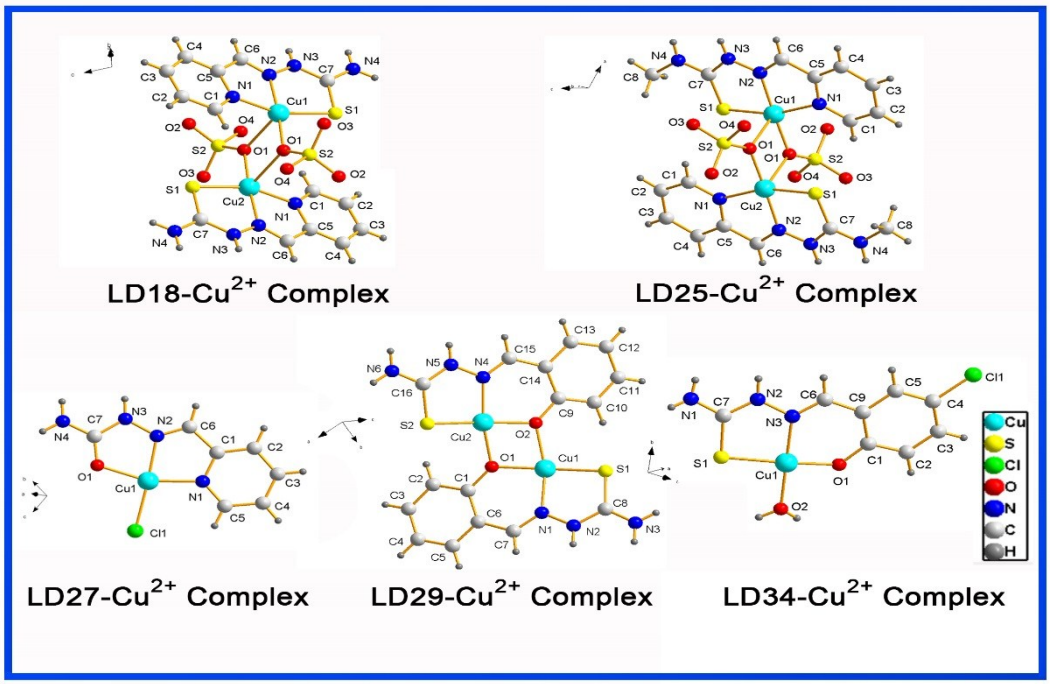

Supporting information Figure 4. Cyclic voltammograms of the Cu^{2+}-chelator complexes at 2.0 mM in anhydrous deoxygenated DMF containing 0.1 M $NaClO_4$ as the supporting electrolyte at a scan rate of 0.05 V/s. Working electrode: glassy carbon; counter electrode: Pt wire; reference electrode: Ag/AgCl.

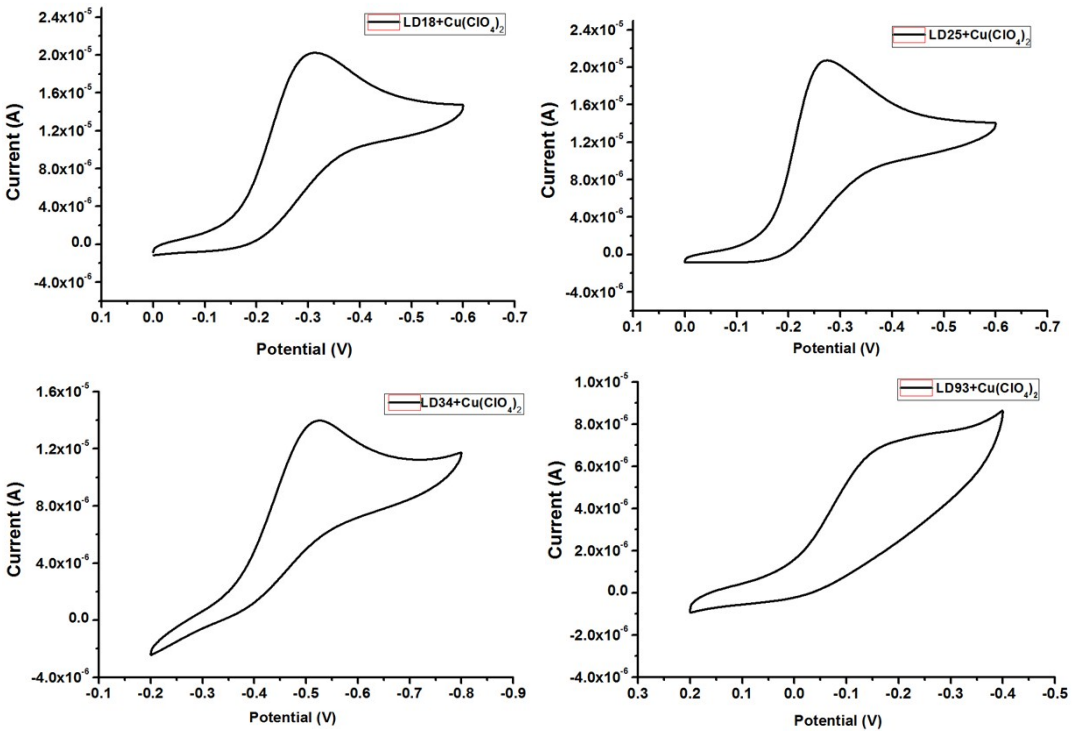

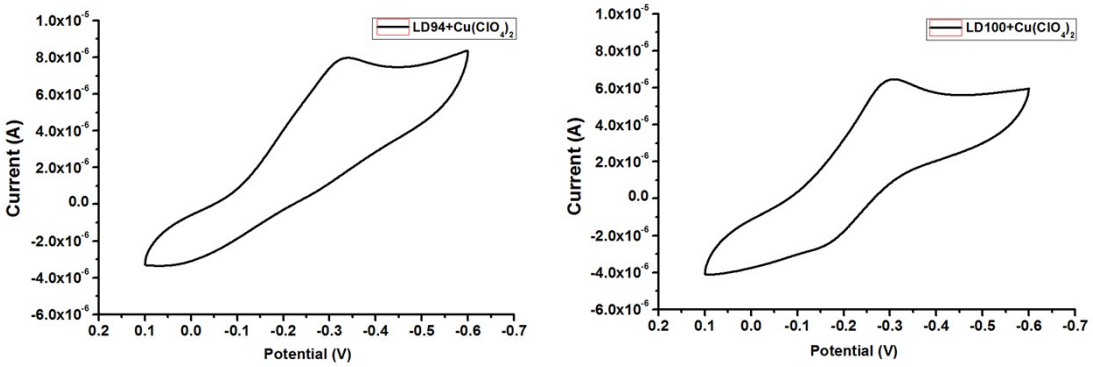

Supporting information Figure 5. The 50% inhibitory concentrations (IC_{50}) of the intracellular SOD1 activity of the inhibitors, TM and ATSM.

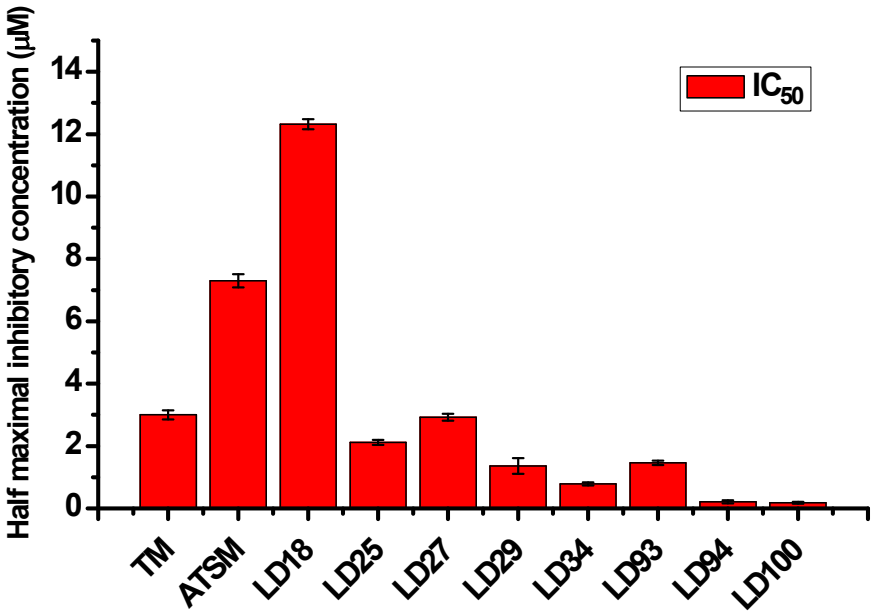

Supporting information Figure 6. Fluorescence anisotropy of 50 µM **LD100** in 20 mM Tris-HCl at pH7.4 with increasing concentration of SOD1. Plots of $lgf_B - \lg(1 - f_B)$ versus $lg\ (C_p - C_L.f_B)$, the X (define $lg\ (C_p - C_L.f_B)$) and Y (define $lgf_B - \lg(1 - f_B)$). The best fit (R^2 = 0.9935, slope is 1.01) gives lgK is 7.28, K = 1.91× 10^7 M^{-1}

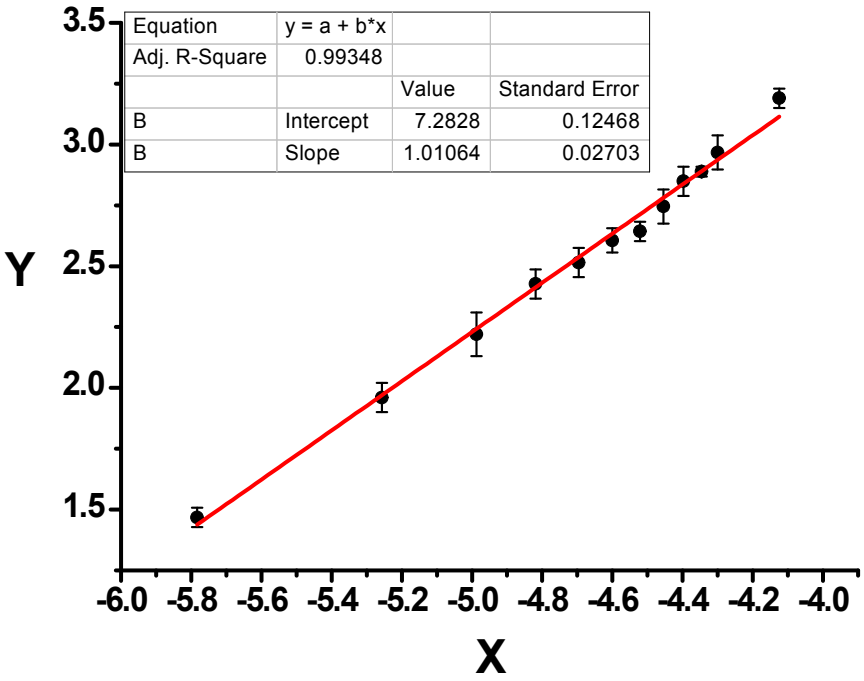

Supporting information Figure 7. RT-PCR assays of the intracellular SOD1 mRNA level. The cells were treated for 24 h with 0.1 – 20 μM **LD18** or **LD94**.

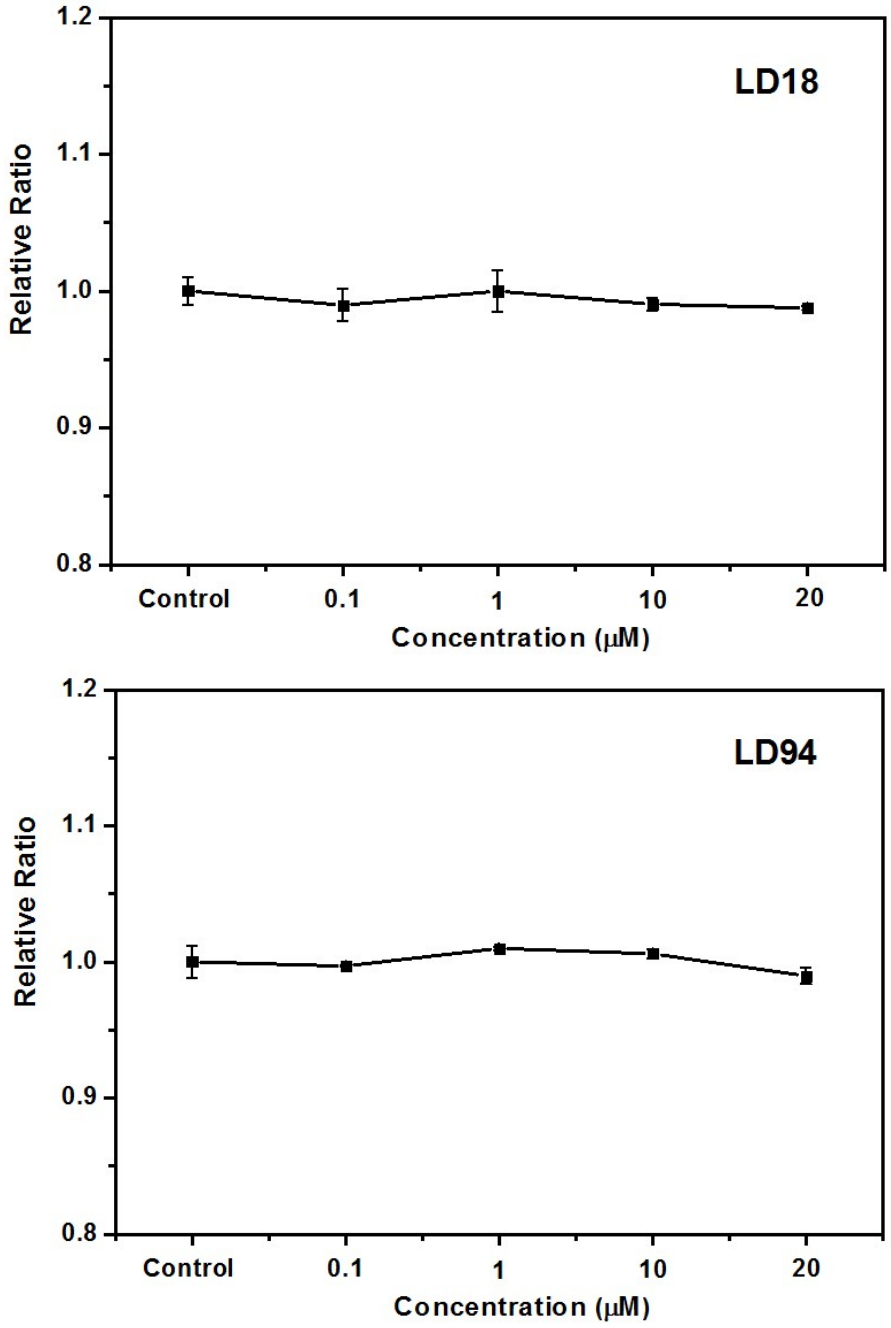

Supporting information Figure 8. CoC activity were measured using UV spectrophotometer in the Du145 cells treated for 24 h with 50 μM SOD1 inhibitors, the control was the solution containing 1% DMSO.

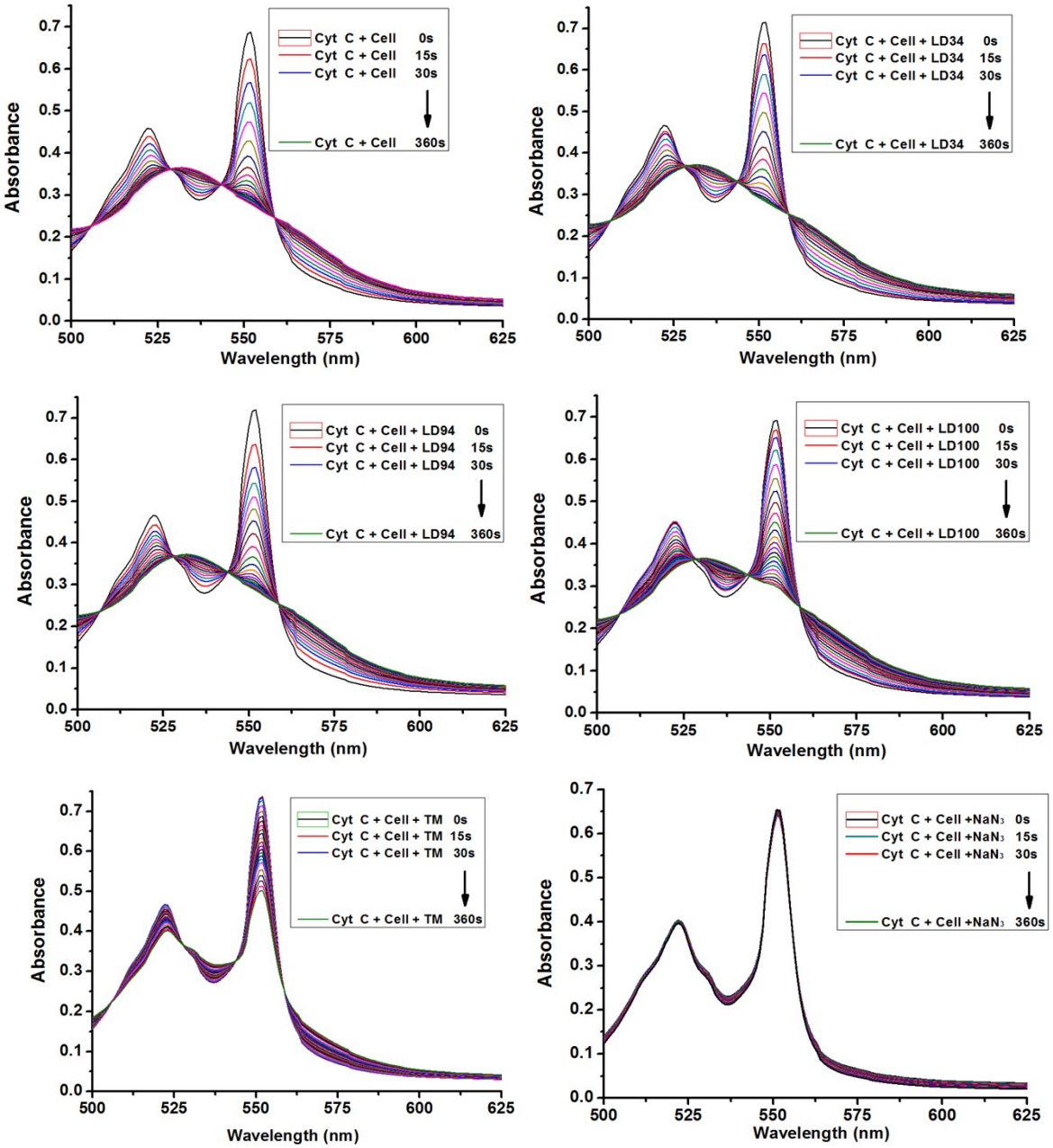

Supporting information Figure 9. Cu(I)-binding proteins/ligands and copper trafficking pathways in the eukaryotic cell.[20]

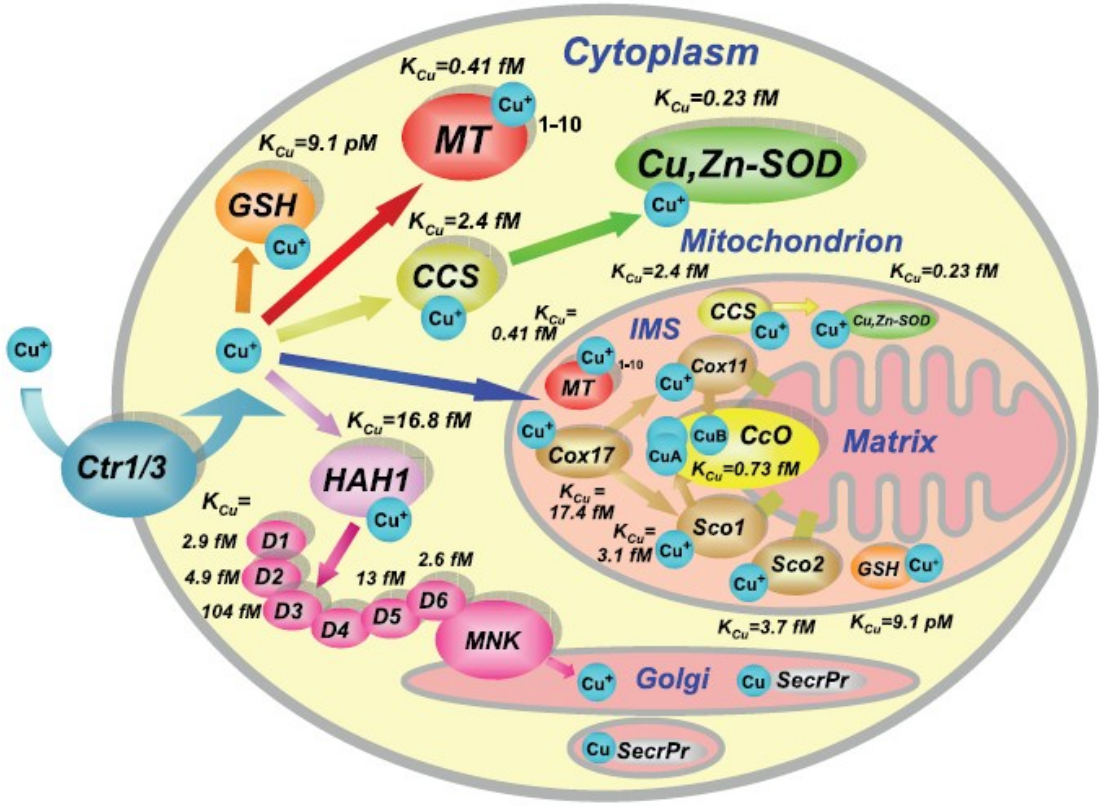

Supporting information 10. The interactions between SOD1 inhibitors (left, **LD34**; right, **LD100**) and tyrosinase molecule displayed by the molecular docking simulation.

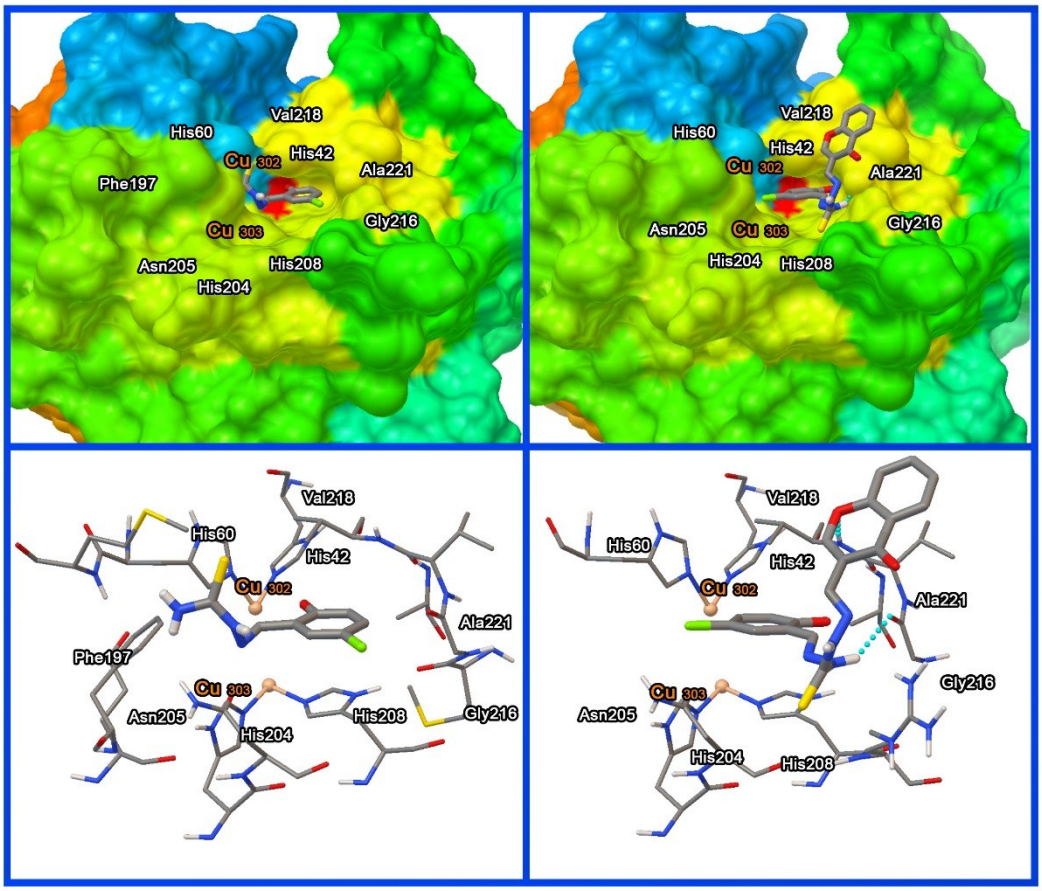
Val218
His60
His42
Cu 302
Ala221
Phe197
Gly216
Cu 303
Asn205
His208
His204
Val218
His60
His42
Cu 302
Ala221
Asn205
Cu 303
Gly216
His204
His208
Val218
His60
His42
Cu 302
Ala221
Phe197
Cu 303
Asn205
His208
Gly216
His204
Val218
His60
His42
Cu 302
Ala221
Gly216
Cu 303
Asn205
His204
His208